in Proc. IEEE ICASSP 2011
Prague, Czech Republic, May 2011, pp. 537-540

P AND T WAVE DELINEATION AND WAVEFORM ESTIMATION IN ECG SIGNALS USING A BLOCK GIBBS SAMPLER

Chao Lin[1], *Georg Kail*[2], *Jean-Yves Tourneret*[1], *Corinne Mailhes*[1], *and Franz Hlawatsch*[2]

[1]University of Toulouse, IRIT/ENSEEIHT/TéSA, 2 rue Charles Camichel, BP 7122, 31071 Toulouse cedex 7, France
[2]Institute of Telecommunications, Gusshausstrasse 25/389, Vienna University of Technology, A-1040 Vienna, Austria
chao.lin@tesa.prd.fr, {jean-yves.tourneret, corinne.mailhes}@enseeiht.fr, {gkail, fhlawats}@nt.tuwien.ac.at

ABSTRACT

The delineation of P and T waves is important for the interpretation of ECG signals. We propose a Bayesian detection-estimation algorithm for simultaneous detection, delineation, and estimation of P and T waves. A block Gibbs sampler exploits the strong local dependencies in ECG signals by imposing block constraints on the P and T wave locations. The proposed algorithm is evaluated on the annotated QT database and compared with two classical algorithms.

Index Terms— ECG, P and T wave delineation, Bayesian analysis, Gibbs sampling, MCMC method.

1. INTRODUCTION

In electrocardiograms (ECGs), most of the clinically useful information can be found in the wave intervals, amplitudes, or morphology. Therefore, efficient and robust methods for automated ECG delineation are of great importance. The QRS complex is relatively easy to detect and is thus generally used as a reference within the cardiac cycle. For P and T wave detection and delineation (i.e., determination of peaks and boundaries of the P and T waves), most existing methods perform QRS detection first. They then define temporal search windows before and after the detected QRS location to search for the P and T waves using filtering [1], basis expansions [2], or thresholding [3]. Because of the low slope and magnitude of the P and T waves, as well as the presence of noise, interference, and baseline fluctuation, P and T wave delineation remains a difficult task. Furthermore, in addition to delineation, accurate estimation of the waveform itself may be important, e.g., for T wave alternans detection [4].

In this paper, we propose a Bayesian model and a detection/estimation method for simultaneous P and T wave delineation and waveform estimation. Our model takes into account prior distributions for the unknown parameters (wave locations and amplitudes as well as waveform and local baseline coefficients). A block Gibbs sampler [5] is used because the Bayesian detector/estimator cannot be calculated in closed form. While a Gibbs-type sampler for P and T wave delineation was recently proposed in [6], a new feature of our sampler is a block constraint on the wave locations that improves convergence and computational efficiency. Further novel contributions are the consideration of a local baseline in each block (which was assumed to be filtered out in [6]) and a dimensionality-reducing expansion of the P and T waveforms into Hermite basis functions.

This paper is organized as follows. Section 2 describes a model for the non-QRS signal components. In Section 3, the prior and posterior distributions of all unknown parameters are discussed. A block Gibbs sampler is proposed in Section 4. Simulation results using the QT database [7] and a comparison with two alternative algorithms are presented in Section 5.

This work was supported by the FWF under grant S10603 (Statistical Inference) within the National Research Network SISE.

2. SIGNAL MODEL FOR THE NON-QRS INTERVALS

Non-QRS intervals in an ECG signal are located between a QRS end and the subsequent QRS onset. The non-QRS interval $\mathcal{J}_n$ associated with the nth heartbeat consists of a T wave interval $\mathcal{J}_{\mathrm{T},n}$, which may contain a T wave, and a P wave interval $\mathcal{J}_{\mathrm{P},n}$, which may contain a P wave. The temporal lengths of $\mathcal{J}_n$, $\mathcal{J}_{\mathrm{T},n}$, and $\mathcal{J}_{\mathrm{P},n}$ will be denoted by N_n, $N_{\mathrm{T},n}$, and $N_{\mathrm{P},n}$, respectively. Here, $N_{\mathrm{T},n}$ and $N_{\mathrm{P},n}$ can be determined by a cardiologist or simply as fixed percentages of N_n. Note that $N_{\mathrm{T},n} + N_{\mathrm{P},n} = N_n$.

Our goal is to estimate the waveforms and amplitudes of the P and T waves and their locations within their respective intervals. The locations of the non-QRS intervals are provided by a prior QRS detection step, which will not be considered here. Due to the nonstationary nature of ECGs, we perform detection and estimation only for a limited set of consecutive beats at once. More specifically, we will consider the beats $n \in \{1, \ldots, D\}$ located within a D-beat processing window of length M (see Fig. 1(a)).

As shown in Fig. 1(b), the signal in each non-QRS interval can be approximated by two pulses representing the P and T waves plus a local baseline. The waveforms of all T pulses within a D-beat processing window are assumed to be equal, whereas their amplitudes

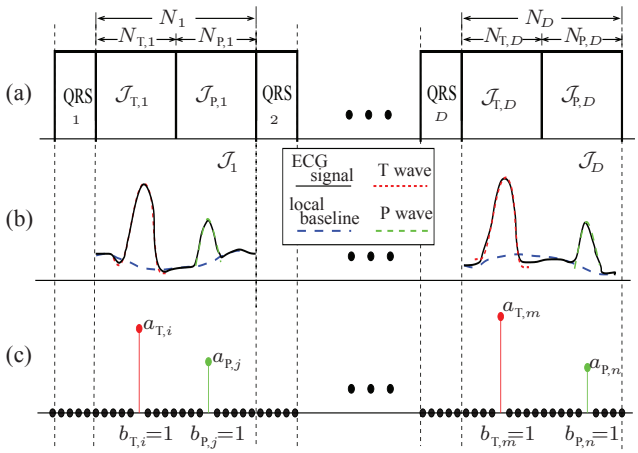

Fig. 1. ECG signal within a D-beat window: (a) QRS and non-QRS intervals (in this example, $N_{\mathrm{T},n} = N_{\mathrm{P},n} = N_n/2$), (b) signal in the non-QRS intervals, (c) impulse sequences $u_{\mathrm{T},k}$ and $u_{\mathrm{P},k}$.

and locations vary with the beat index n. Thus, the T waves within a window can be modeled by the convolution of the unknown T waveform $\boldsymbol{h}_{\mathrm{T}} = (h_{\mathrm{T},0} \cdots h_{\mathrm{T},L})^T$ with an unknown "impulse" sequence $\boldsymbol{u}_{\mathrm{T}} = (u_{\mathrm{T},1} \cdots u_{\mathrm{T},M})^T$ indicating the T wave locations and amplitudes (see Fig. 1(c)). Note that at most D entries of $\boldsymbol{u}_{\mathrm{T}}$ are nonzero; each of these "impulses" corresponds to one T wave. Similarly, the P waves within a window are modeled by the convolution of $\boldsymbol{h}_{\mathrm{P}} = (h_{\mathrm{P},0} \cdots h_{\mathrm{P},L})^T$ with $\boldsymbol{u}_{\mathrm{P}} = (u_{\mathrm{P},1} \cdots u_{\mathrm{P},M})^T$. Let $\mathcal{J}$ be the union of all T and P wave intervals $\mathcal{J}_{\mathrm{T},n}$ and $\mathcal{J}_{\mathrm{P},n}$ within the window considered, and let $K \triangleq |\mathcal{J}|$ be the corresponding signal length. The non-QRS signal component can then be written as

$$x_k = \sum_{l=0}^{L} h_{\mathrm{T},l}\, u_{\mathrm{T},k-l} + \sum_{l=0}^{L} h_{\mathrm{P},l}\, u_{\mathrm{P},k-l} + c_k + w_k\,, \quad k \in \mathcal{J}, \quad (1)$$

where c_k denotes the baseline sequence and w_k denotes white Gaussian noise with unknown variance σ_w^2. Note that we assume that $u_{\mathrm{T},k} = u_{\mathrm{P},k} = 0$ for $k \notin \mathcal{J}$.

We propose to represent the P and T waveforms by a basis expansion using discrete-time versions of the first G Hermite functions (cf. [8–10]). Thus, the waveform vectors can be written as

$$\boldsymbol{h}_{\mathrm{T}} = \boldsymbol{H}\boldsymbol{\alpha}_{\mathrm{T}}\,, \quad \boldsymbol{h}_{\mathrm{P}} = \boldsymbol{H}\boldsymbol{\alpha}_{\mathrm{P}}\,, \quad (2)$$

where $\boldsymbol{H}$ is an $(L+1) \times G$ matrix whose columns are the first G Hermite functions (with $G \leq L+1$), suitably sampled and truncated to length $L+1$, and $\boldsymbol{\alpha}_{\mathrm{T}}$ and $\boldsymbol{\alpha}_{\mathrm{P}}$ are unknown coefficient vectors of length G. Furthermore, the local baseline within the nth non-QRS interval $\mathcal{J}_n$ is modeled by a 4th-degree polynomial, i.e.,

$$c_{n,k} = \sum_{i=1}^{5} \gamma_{n,i}\, k^{i-1}, \quad k = 1, \ldots, N_n\,, \quad (3)$$

for each $n \in \{1, \ldots, D\}$. This local baseline model extends that of [11], which assumes that the local baseline is constant in $\mathcal{J}_n$ (i.e., $\gamma_{n,i} = 0$ for $i \geq 2$). In vector-matrix form, (3) reads as $\boldsymbol{c}_n = \boldsymbol{M}_n\boldsymbol{\gamma}_n$, with the known $N_n \times 5$ Vandermonde matrix $\boldsymbol{M}_n$ and the unknown coefficient vector $\boldsymbol{\gamma}_n = (\gamma_{n,1} \cdots \gamma_{n,5})^T$. The baseline sequence for the entire D-beat window can then be written as

$$\boldsymbol{c} = \boldsymbol{M}\boldsymbol{\gamma}\,, \quad (4)$$

where $\boldsymbol{c}$, $\boldsymbol{M}$, and $\boldsymbol{\gamma}$ are obtained by suitably stacking the $\boldsymbol{c}_n$, $\boldsymbol{M}_n$, and $\boldsymbol{\gamma}_n$, respectively, for $n = 1, \ldots, D$. Using (2) and (4), we obtain the following vector representation of the non-QRS signal in (1):

$$\boldsymbol{x} = \boldsymbol{F}_{\mathrm{T}}\boldsymbol{u}_{\mathrm{T}} + \boldsymbol{F}_{\mathrm{P}}\boldsymbol{u}_{\mathrm{P}} + \boldsymbol{M}\boldsymbol{\gamma} + \boldsymbol{w}\,. \quad (5)$$

Here, $\boldsymbol{F}_{\mathrm{T}}$ is the $K \times M$ Toeplitz matrix with first row $\begin{pmatrix}\boldsymbol{h}_1^T\boldsymbol{\alpha}_{\mathrm{T}} & \boldsymbol{0}_{M-1}^T\end{pmatrix}$, where $\boldsymbol{h}_1^T$ is the first row of the matrix $\boldsymbol{H}$ and $\boldsymbol{0}_{M-1}$ is the zero vector of length $M-1$, and with first column $\begin{pmatrix}(\boldsymbol{H}\boldsymbol{\alpha}_{\mathrm{T}})^T & \boldsymbol{0}_{M-1}^T\end{pmatrix}^T$. $\boldsymbol{F}_{\mathrm{P}}$ is defined similarly, with $\boldsymbol{\alpha}_{\mathrm{T}}$ replaced by $\boldsymbol{\alpha}_{\mathrm{P}}$.

The proposed detection-estimation method is based on writing the impulse sequences as products $u_{\mathrm{T},k} = b_{\mathrm{T},k}\, a_{\mathrm{T},k}$ ($u_{\mathrm{P},k} = b_{\mathrm{P},k}\, a_{\mathrm{P},k}$) of binary indicator sequences $b_{\mathrm{T},k} \in \{0,1\}$ ($b_{\mathrm{P},k} \in \{0,1\}$) and amplitude factors $a_{\mathrm{T},k} \in \mathbb{R}$ ($a_{\mathrm{P},k} \in \mathbb{R}$). Each $b_{\mathrm{T},k} = 1$ ($b_{\mathrm{P},k} = 1$) indicates the location of a T wave (P wave), and the corresponding $a_{\mathrm{T},k}$ ($a_{\mathrm{P},k}$) is the respective amplitude. Note that the $a_{\mathrm{T},k}$ ($a_{\mathrm{P},k}$) are undefined for all k where $b_{\mathrm{T},k} = 0$ ($b_{\mathrm{P},k} = 0$). Let $\boldsymbol{b}_{\mathrm{T}}$, $\boldsymbol{b}_{\mathrm{P}}$, $\boldsymbol{a}_{\mathrm{T}}$, and $\boldsymbol{a}_{\mathrm{P}}$ denote the length-M vectors corresponding to $b_{\mathrm{T},k}$, $b_{\mathrm{P},k}$, $a_{\mathrm{T},k}$, and $a_{\mathrm{P},k}$, respectively. Then (5) can be rewritten as

$$\boldsymbol{x} = \boldsymbol{F}_{\mathrm{T}}\boldsymbol{B}_{\mathrm{T}}\boldsymbol{a}_{\mathrm{T}} + \boldsymbol{F}_{\mathrm{P}}\boldsymbol{B}_{\mathrm{P}}\boldsymbol{a}_{\mathrm{P}} + \boldsymbol{M}\boldsymbol{\gamma} + \boldsymbol{w}\,, \quad (6)$$

with the diagonal $M \times M$ matrices $\boldsymbol{B}_{\mathrm{T}} \triangleq \mathrm{diag}(\boldsymbol{b}_{\mathrm{T}})$ and $\boldsymbol{B}_{\mathrm{P}} \triangleq \mathrm{diag}(\boldsymbol{b}_{\mathrm{P}})$.

3. BAYESIAN MODEL

The unknown parameter vector resulting from the above parametrization is $\boldsymbol{\theta} = (\boldsymbol{\theta}_{\mathrm{T}}^T\ \boldsymbol{\theta}_{\mathrm{P}}^T\ \boldsymbol{\theta}_{\mathrm{cw}}^T)^T$, where $\boldsymbol{\theta}_{\mathrm{T}} \triangleq (\boldsymbol{b}_{\mathrm{T}}^T\ \boldsymbol{a}_{\mathrm{T}}^T\ \boldsymbol{\alpha}_{\mathrm{T}}^T)^T$ and $\boldsymbol{\theta}_{\mathrm{P}} \triangleq (\boldsymbol{b}_{\mathrm{P}}^T\ \boldsymbol{a}_{\mathrm{P}}^T\ \boldsymbol{\alpha}_{\mathrm{P}}^T)^T$ are related to the T and P wave, respectively and $\boldsymbol{\theta}_{\mathrm{cw}} \triangleq (\boldsymbol{\gamma}^T\ \sigma_w^2)^T$ is related to the baseline and noise. Bayesian detection/estimation relies on the posterior distribution $p(\boldsymbol{\theta}|\boldsymbol{x}) \propto p(\boldsymbol{x}|\boldsymbol{\theta})p(\boldsymbol{\theta})$ (here, $\propto$ means "proportional to"), where $p(\boldsymbol{x}|\boldsymbol{\theta})$ is the likelihood function and $p(\boldsymbol{\theta})$ is the prior distribution of $\boldsymbol{\theta}$.

Likelihood function. Using our model (6) and the fact that w_k is white Gaussian noise, the likelihood function is obtained as

$$p(\boldsymbol{x}|\boldsymbol{\theta}) \propto \frac{1}{\sigma_w^K} \exp\!\left(-\frac{1}{2\sigma_w^2}\left\|\boldsymbol{x} - \boldsymbol{F}_{\mathrm{T}}\boldsymbol{B}_{\mathrm{T}}\boldsymbol{a}_{\mathrm{T}} - \boldsymbol{F}_{\mathrm{P}}\boldsymbol{B}_{\mathrm{P}}\boldsymbol{a}_{\mathrm{P}} - \boldsymbol{M}\boldsymbol{\gamma}\right\|^2\right),$$

where $\|\cdot\|$ is the ℓ_2 norm, i.e., $\|\boldsymbol{x}\|^2 = \boldsymbol{x}^T\boldsymbol{x}$.

Prior distribution. Since there are no known relations between $(\boldsymbol{b}_{\mathrm{T}}, \boldsymbol{a}_{\mathrm{T}})$, $(\boldsymbol{b}_{\mathrm{P}}, \boldsymbol{a}_{\mathrm{P}})$, $\boldsymbol{\alpha}_{\mathrm{T}}$, $\boldsymbol{\alpha}_{\mathrm{P}}$, $\boldsymbol{\gamma}$, and σ_w^2, all these sets of parameters are modeled as *a priori* statistically independent of each other. We will now discuss the prior distributions of these parameters. Let $\boldsymbol{b}_{\mathcal{J}_{\mathrm{T},n}}$, $n \in \{1, \ldots, D\}$ comprise all entries of the T wave indicator vector $\boldsymbol{b}_{\mathrm{T}}$ that are indexed by the T wave interval $\mathcal{J}_{\mathrm{T},n}$. The indicators are subject to a *block constraint*: within $\mathcal{J}_{\mathrm{T},n}$, there is one T wave (thus, $\|\boldsymbol{b}_{\mathcal{J}_{\mathrm{T},n}}\| = 1$) or none (thus, $\|\boldsymbol{b}_{\mathcal{J}_{\mathrm{T},n}}\| = 0$), the latter case being very unlikely. Therefore, we define the prior of $\boldsymbol{b}_{\mathcal{J}_{\mathrm{T},n}}$ as

$$p(\boldsymbol{b}_{\mathcal{J}_{\mathrm{T},n}}) = \begin{cases} p_0 & \text{if } \|\boldsymbol{b}_{\mathcal{J}_{\mathrm{T},n}}\| = 0 \\ p_1 & \text{if } \|\boldsymbol{b}_{\mathcal{J}_{\mathrm{T},n}}\| = 1 \\ 0 & \text{otherwise,} \end{cases} \quad (7)$$

where $p_1 = (1-p_0)/N_{\mathrm{T},n}$ and p_0 is chosen very small. The $\boldsymbol{b}_{\mathcal{J}_{\mathrm{T},n}}$ (for different n) are statistically independent of each other, and all remaining entries of the total vector $\boldsymbol{b}_{\mathrm{T}}$ (i.e., entries outside the T wave intervals $\mathcal{J}_{\mathrm{T},n}$) are zero. Thus, the prior of $\boldsymbol{b}_{\mathrm{T}}$ is given by

$$p(\boldsymbol{b}_{\mathrm{T}}) = \prod_{n=1}^{D} p(\boldsymbol{b}_{\mathcal{J}_{\mathrm{T},n}})\,.$$

For the T wave amplitudes $a_{\mathrm{T},k}$ at those k where $b_{\mathrm{T},k} = 1$ (recall that the $a_{\mathrm{T},k}$ are undefined otherwise), we choose a zero-mean Gaussian prior, i.e., $p(a_{\mathrm{T},k}|b_{\mathrm{T},k}=1) = \mathcal{N}(a_{\mathrm{T},k}; 0, \sigma_a^2)$. This allows for both positive and negative amplitudes. Amplitudes $a_{\mathrm{T},k}|b_{\mathrm{T},k}=1$ at different k are modeled as statistically independent. It follows that $u_{\mathrm{T},k} = b_{\mathrm{T},k}\, a_{\mathrm{T},k}$ is a Bernoulli-Gaussian sequence with block constraints.

The priors of the P wave indicators $b_{\mathrm{P},k}$ and amplitudes $a_{\mathrm{P},k}$ are defined in a fully analogous way, with the same fixed hyperparameters p_0, p_1, and σ_a^2. Furthermore, the P wave variables are modeled as independent of the T wave variables.

The T waveform coefficients are modeled as independent and identically distributed (iid), zero-mean, and Gaussian, i.e., $p(\boldsymbol{\alpha}_{\mathrm{T}}) = \mathcal{N}(\boldsymbol{\alpha}_{\mathrm{T}}; \boldsymbol{0}, \sigma_\alpha^2\mathbf{I}_{L+1})$, where $\mathbf{I}_{L+1}$ denotes the identity matrix of size $(L+1) \times (L+1)$. The same prior is chosen for the P wave coefficients, i.e., $p(\boldsymbol{\alpha}_{\mathrm{P}}) = \mathcal{N}(\boldsymbol{\alpha}_{\mathrm{P}}; \boldsymbol{0}, \sigma_\alpha^2\mathbf{I}_{L+1})$.

The baseline coefficients $\gamma_{n,i}$ are also modeled as iid zero-mean Gaussian, i.e., $p(\boldsymbol{\gamma}) = \mathcal{N}(\boldsymbol{\gamma}; \boldsymbol{0}, \sigma_\gamma^2\mathbf{I}_{5D})$. The variances σ_a^2, σ_α^2, and σ_γ^2 are fixed hyperparameters; more specifically, we choose $\sigma_a^2 = 1$ (since the ECG signals are normalized by their maximum R-peak amplitude) and $\sigma_\alpha^2 = 1$ (normalization of the waveform amplitude, to avoid scale ambiguity). Finally, the noise variance σ_w^2 is modeled as a random hyperparameter with inverse gamma distribution $\mathcal{IG}\left(\sigma_w^2; \xi, \eta\right)$, where ξ and η are fixed hyperparameters providing a

vague prior [12]. Our choice of conjugate priors for $\boldsymbol{\alpha}_{\mathrm{T}}$, $\boldsymbol{\alpha}_{\mathrm{P}}$, $\boldsymbol{\gamma}$, and σ_w^2 considerably simplifies our algorithm since the resulting posterior distributions are also Gaussian and inverse gamma, respectively.

Posterior distribution. The posterior distribution of the parameter vector $\boldsymbol{\theta}$ is given by

$$p(\boldsymbol{\theta}|\boldsymbol{x}) \propto p(\boldsymbol{x}|\boldsymbol{\theta})p(\boldsymbol{\theta}) = p(\boldsymbol{x}|\boldsymbol{\theta})p(\boldsymbol{\theta}_{\mathrm{T}})p(\boldsymbol{\theta}_{\mathrm{P}})p(\boldsymbol{\theta}_{\mathrm{cw}}), \quad (8)$$

with $p(\boldsymbol{\theta}_{\mathrm{T}}) = p(\boldsymbol{a}_{\mathrm{T}}|\boldsymbol{b}_{\mathrm{T}})p(\boldsymbol{b}_{\mathrm{T}})p(\boldsymbol{\alpha}_{\mathrm{T}})$, $p(\boldsymbol{\theta}_{\mathrm{P}}) = p(\boldsymbol{a}_{\mathrm{P}}|\boldsymbol{b}_{\mathrm{P}})p(\boldsymbol{b}_{\mathrm{P}})p(\boldsymbol{\alpha}_{\mathrm{P}})$, and $p(\boldsymbol{\theta}_{\mathrm{cw}}) = p(\boldsymbol{\gamma})p(\sigma_w^2)$. Due to the complexity of this distribution, we propose to use a block Gibbs sampler that generates samples asymptotically distributed according to $p(\boldsymbol{\theta}|\boldsymbol{x})$. From these samples, the discrete parameters $\boldsymbol{b}_{\mathrm{T}}$ and $\boldsymbol{b}_{\mathrm{P}}$ are then detected by means of the sample-based maximum a posteriori detector, and the continuous parameters $\boldsymbol{a}_{\mathrm{T}}$, $\boldsymbol{a}_{\mathrm{P}}$, $\boldsymbol{\alpha}_{\mathrm{T}}$, $\boldsymbol{\alpha}_{\mathrm{P}}$, $\boldsymbol{\gamma}$, and σ_w^2 are estimated by means of the sample-based minimum mean square error estimator.

4. BLOCK GIBBS SAMPLER

The proposed block Gibbs sampler is summarized in Algorithm 1. The sampling distributions involved are the full conditional distributions of $p(\boldsymbol{\theta}|\boldsymbol{x})$ defined in (8) and are detailed below. The sampling distributions of the P wave parameters $\boldsymbol{\theta}_{\mathrm{P}}$ are similar to those of $\boldsymbol{\theta}_{\mathrm{T}}$; they are omitted because of space limitations. We note that $\boldsymbol{b}_{\sim\mathcal{J}_{\mathrm{T},n}}$ denotes $\boldsymbol{b}_{\mathrm{T}}$ without the entries indexed by $\mathcal{J}_{\mathrm{T},n}$, and similarly for $\boldsymbol{a}_{\sim\mathcal{J}_{\mathrm{T},n}}$. To see that the proposed algorithm is a valid Gibbs sampler, note that the sampling steps for $\boldsymbol{b}_{\mathcal{J}_{\mathrm{T},n}}$ and $\boldsymbol{a}_{\mathcal{J}_{\mathrm{T},n}}$ are equivalent to jointly sampling $(\boldsymbol{b}_{\mathcal{J}_{\mathrm{T},n}}, \boldsymbol{a}_{\mathcal{J}_{\mathrm{T},n}})$ from $p(\boldsymbol{b}_{\mathcal{J}_{\mathrm{T},n}}, \boldsymbol{a}_{\mathcal{J}_{\mathrm{T},n}}|\boldsymbol{\theta}_{\sim\mathcal{J}_{\mathrm{T},n}}, \boldsymbol{\theta}_{\mathrm{P}}, \boldsymbol{\theta}_{\mathrm{cw}}, \boldsymbol{x})$, where $\boldsymbol{\theta}_{\sim\mathcal{J}_{\mathrm{T},n}} \triangleq \left(\boldsymbol{b}_{\sim\mathcal{J}_{\mathrm{T},n}}^T\, \boldsymbol{a}_{\sim\mathcal{J}_{\mathrm{T},n}}^T\, \boldsymbol{\alpha}_{\mathrm{T}}^T\right)^T$.

T wave indicators. The sampling distribution for $\boldsymbol{b}_{\mathcal{J}_{\mathrm{T},n}}$ is

$$p(\boldsymbol{b}_{\mathcal{J}_{\mathrm{T},n}}|\boldsymbol{\theta}_{\sim\mathcal{J}_{\mathrm{T},n}}, \boldsymbol{\theta}_{\mathrm{P}}, \boldsymbol{\theta}_{\mathrm{cw}}, \boldsymbol{x}) \propto \sigma_1 \exp\left(\frac{\mu_1^2}{2\sigma_1^2}\right) p(\boldsymbol{b}_{\mathcal{J}_{\mathrm{T},n}}), \quad (9)$$

with

$$\mu_1 = \frac{\sigma_1^2 \boldsymbol{b}_{\mathcal{J}_{\mathrm{T},n}}^T \boldsymbol{F}_{\mathcal{J}_{\mathrm{T},n}}^T}{\sigma_w^2}\left(\boldsymbol{x}_{\mathrm{T}} - \boldsymbol{F}_{\sim\mathcal{J}_{\mathrm{T},n}} \boldsymbol{B}_{\sim\mathcal{J}_{\mathrm{T},n}} \boldsymbol{a}_{\sim\mathcal{J}_{\mathrm{T},n}}\right)$$

$$\sigma_1^2 = \left(\frac{\left\|\boldsymbol{F}_{\mathcal{J}_{\mathrm{T},n}} \boldsymbol{b}_{\mathcal{J}_{\mathrm{T},n}}\right\|^2}{\sigma_w^2} + \frac{1}{\sigma_a^2}\right)^{-1},$$

where $\boldsymbol{F}_{\mathcal{J}_{\mathrm{T},n}}$ contains the columns of $\boldsymbol{F}_{\mathrm{T}}$ indexed by $\mathcal{J}_{\mathrm{T},n}$, $\boldsymbol{F}_{\sim\mathcal{J}_{\mathrm{T},n}}$ is $\boldsymbol{F}_{\mathrm{T}}$ without those columns, $\boldsymbol{x}_{\mathrm{T}} \triangleq \boldsymbol{x} - \boldsymbol{F}_{\mathrm{P}}\boldsymbol{B}_{\mathrm{P}}\boldsymbol{a}_{\mathrm{P}} - \boldsymbol{M}\boldsymbol{\gamma}$, and $\boldsymbol{B}_{\sim\mathcal{J}_{\mathrm{T},n}} \triangleq \mathrm{diag}(\boldsymbol{b}_{\sim\mathcal{J}_{\mathrm{T},n}})$. The sampler evaluates all hypotheses of $\boldsymbol{b}_{\mathcal{J}_{\mathrm{T},n}}$ conditioned on the samples of all other parameters. There are $N_{\mathrm{T},n}+1$ such hypotheses, because $\boldsymbol{b}_{\mathcal{J}_{\mathrm{T},n}}$ has either no 1-entry or exactly one 1-entry at one of $N_{\mathrm{T},n}$ possible locations (cf. the prior in (7)).

T wave amplitudes. The sampling distribution for the $a_{\mathrm{T},k}$ is

$$p(a_{\mathrm{T},k}|b_{\mathrm{T},k}=1, \boldsymbol{\theta}_{\sim\mathcal{J}_{\mathrm{T},n}}, \boldsymbol{\theta}_{\mathrm{P}}, \boldsymbol{\theta}_{\mathrm{cw}}, \boldsymbol{x}) = \mathcal{N}(a_{\mathrm{T},k}; \mu_1, \sigma_1^2). \quad (10)$$

T waveform coefficients. The sampling distribution for $\boldsymbol{\alpha}_{\mathrm{T}}$ is

$$p(\boldsymbol{\alpha}_{\mathrm{T}}|\boldsymbol{b}_{\mathrm{T}}, \boldsymbol{a}_{\mathrm{T}}, \boldsymbol{\theta}_{\mathrm{P}}, \boldsymbol{\theta}_{\mathrm{cw}}, \boldsymbol{x}) = \mathcal{N}(\boldsymbol{\alpha}_{\mathrm{T}}; \boldsymbol{\mu}_2, \boldsymbol{\Sigma}_2), \quad (11)$$

with

$$\boldsymbol{\mu}_2 = \frac{\boldsymbol{\Sigma}_2 \boldsymbol{H}^T \boldsymbol{U}_{\mathrm{T}}^T}{\sigma_w^2}\boldsymbol{x}_{\mathrm{T}}, \quad \boldsymbol{\Sigma}_2 = \left(\frac{\boldsymbol{H}^T \boldsymbol{U}_{\mathrm{T}}^T \boldsymbol{U}_{\mathrm{T}} \boldsymbol{H}}{\sigma_w^2} + \frac{\mathbf{I}_{L+1}}{\sigma_\alpha^2}\right)^{-1}.$$

Algorithm 1 Block Gibbs sampler

for $n = 1, \ldots, D$ **do**
  Sample the block $\boldsymbol{b}_{\mathcal{J}_{\mathrm{T},n}} \sim p(\boldsymbol{b}_{\mathcal{J}_{\mathrm{T},n}}|\boldsymbol{\theta}_{\sim\mathcal{J}_{\mathrm{T},n}}, \boldsymbol{\theta}_{\mathrm{P}}, \boldsymbol{\theta}_{\mathrm{cw}}, \boldsymbol{x})$ (see (9))
  for $k \in \mathcal{J}_{\mathrm{T},n}$ **do**
    if $b_{\mathrm{T},k} = 1$ **then**
      Sample $a_{\mathrm{T},k} \sim p(a_{\mathrm{T},k}|b_{\mathrm{T},k}=1, \boldsymbol{\theta}_{\sim\mathcal{J}_{\mathrm{T},n}}, \boldsymbol{\theta}_{\mathrm{P}}, \boldsymbol{\theta}_{\mathrm{cw}}, \boldsymbol{x})$ (see (10))
    end if
  end for
  Sample the block $\boldsymbol{b}_{\mathcal{J}_{\mathrm{P},n}}$ from $p(\boldsymbol{b}_{\mathcal{J}_{\mathrm{P},n}}|\boldsymbol{\theta}_{\sim\mathcal{J}_{\mathrm{P},n}}, \boldsymbol{\theta}_{\mathrm{T}}, \boldsymbol{\theta}_{\mathrm{cw}}, \boldsymbol{x})$
  for $k \in \mathcal{J}_{\mathrm{P},n}$ **do**
    if $b_{\mathrm{P},k} = 1$ **then**
      Sample $a_{\mathrm{P},k} \sim p(a_{\mathrm{P},k}|b_{\mathrm{P},k}=1, \boldsymbol{\theta}_{\sim\mathcal{J}_{\mathrm{P},n}}, \boldsymbol{\theta}_{\mathrm{T}}, \boldsymbol{\theta}_{\mathrm{cw}}, \boldsymbol{x})$
    end if
  end for
end for
Sample $\boldsymbol{\alpha}_{\mathrm{T}}$ from $p(\boldsymbol{\alpha}_{\mathrm{T}}|\boldsymbol{b}_{\mathrm{T}}, \boldsymbol{a}_{\mathrm{T}}, \boldsymbol{\theta}_{\mathrm{P}}, \boldsymbol{\theta}_{\mathrm{cw}}, \boldsymbol{x})$ (see (11))
Sample $\boldsymbol{\alpha}_{\mathrm{P}}$ from $p(\boldsymbol{\alpha}_{\mathrm{P}}|\boldsymbol{b}_{\mathrm{P}}, \boldsymbol{a}_{\mathrm{P}}, \boldsymbol{\theta}_{\mathrm{T}}, \boldsymbol{\theta}_{\mathrm{cw}}, \boldsymbol{x})$
Sample $\boldsymbol{\gamma}$ from $p(\boldsymbol{\gamma}|\boldsymbol{\theta}_{\mathrm{T}}, \boldsymbol{\theta}_{\mathrm{P}}, \sigma_w^2, \boldsymbol{x})$ (see (12))
Sample σ_w^2 from $p(\sigma_w^2|\boldsymbol{\theta}_{\mathrm{T}}, \boldsymbol{\theta}_{\mathrm{P}}, \boldsymbol{\gamma}, \boldsymbol{x})$ (see (13))

Here, $\boldsymbol{U}_{\mathrm{T}}$ is the Toeplitz matrix of size $K \times (L+1)$ with first row $(u_{\mathrm{T},1}\ \mathbf{0}_L^T)$ and first column $(\boldsymbol{u}_{\mathrm{T}}^T\ \mathbf{0}_L^T)^T$.

Local baseline coefficients. The sampling distribution for $\boldsymbol{\gamma}$ is

$$p(\boldsymbol{\gamma}|\boldsymbol{\theta}_{\mathrm{T}}, \boldsymbol{\theta}_{\mathrm{P}}, \sigma_w^2, \boldsymbol{x}) = \mathcal{N}(\boldsymbol{\gamma}; \boldsymbol{\mu}_3, \boldsymbol{\Sigma}_3), \quad (12)$$

with

$$\boldsymbol{\mu}_3 = \frac{\boldsymbol{\Sigma}_3 \boldsymbol{M}^T}{\sigma_w^2}\boldsymbol{x}_{\boldsymbol{\gamma}}, \quad \boldsymbol{\Sigma}_3 = \left(\frac{\boldsymbol{M}^T\boldsymbol{M}}{\sigma_w^2} + \frac{\mathbf{I}_{5D}}{\sigma_\gamma^2}\right)^{-1},$$

where $\boldsymbol{x}_{\boldsymbol{\gamma}} \triangleq \boldsymbol{x} - \boldsymbol{F}_{\mathrm{T}}\boldsymbol{B}_{\mathrm{T}}\boldsymbol{a}_{\mathrm{T}} - \boldsymbol{F}_{\mathrm{P}}\boldsymbol{B}_{\mathrm{P}}\boldsymbol{a}_{\mathrm{P}}$.

Noise variance. The sampling distribution for σ_w^2 is

$$p(\sigma_w^2|\boldsymbol{\theta}_{\mathrm{T}}, \boldsymbol{\theta}_{\mathrm{P}}, \boldsymbol{\gamma}, \boldsymbol{x}) = \mathcal{IG}(\sigma_w^2; \xi', \eta'), \quad (13)$$

with $\xi' = \xi + \frac{K}{2}$ and $\eta' = \eta + \frac{1}{2}\|\boldsymbol{x} - \boldsymbol{F}_{\mathrm{T}}\boldsymbol{B}_{\mathrm{T}}\boldsymbol{a}_{\mathrm{T}} - \boldsymbol{F}_{\mathrm{P}}\boldsymbol{B}_{\mathrm{P}}\boldsymbol{a}_{\mathrm{P}} - \boldsymbol{M}\boldsymbol{\gamma}\|^2$.

5. SIMULATION RESULTS

We evaluated the performance of the proposed algorithm on the QT database (QTDB) [7]. The QTDB contains 105 15-minute excerpts of two-channel Holter recordings from several widely used ECG databases, chosen to include a variety of P and T wave morphologies. In a preprocessing step, the QRS complexes were detected using the algorithm proposed in [13]. Based on the detected QRS-complex locations, P and T wave search intervals were then defined.

Fig. 2(a) shows an ECG signal segment from the QTDB dataset sele0136. Corresponding estimates—produced by our algorithm—of the marginal posterior probabilities of having a P or T wave at a given location are shown in Fig. 2(b). (We note that the maximum a posteriori detector used in our algorithm detects a wave at a given location if the respective posterior probability estimate is above $1/2$.) Fig. 2(c) shows the estimated T and P waveforms for the 10-beat window considered (i.e., $D = 10$). The wave onsets and ends were determined by searching for the first negative local minimum on ei-

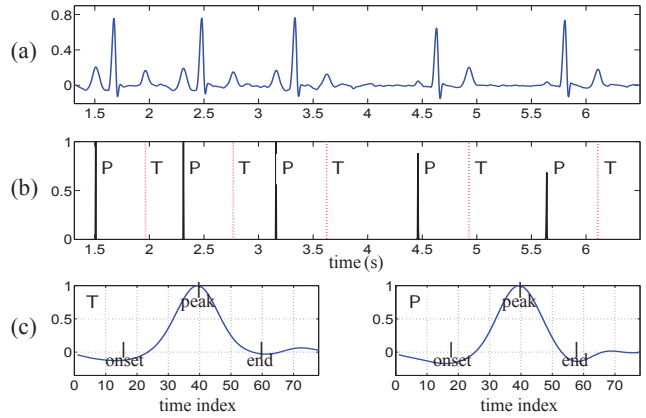

Fig. 2. (a) Segment of an ECG signal. (b) Posterior probabilities of the occurrence of P waves (black solid line) and T waves (red dotted line). (c) Estimated T and P waveforms (normalized).

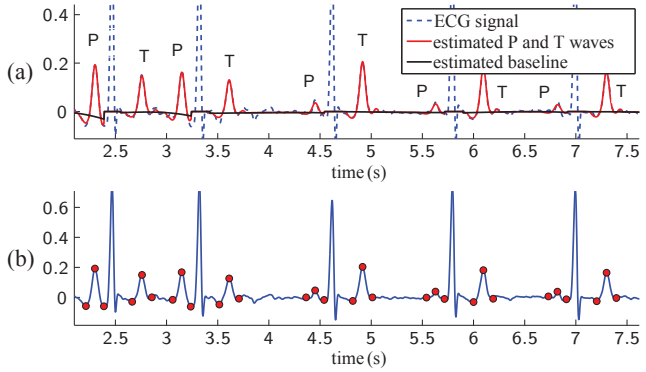

Fig. 3. (a) ECG signal segment (dashed blue), estimated local baseline (black), and estimated P and T waves (red). (b) Results of P and T wave delineation.

ther side of the wave peak. Fig. 3(a) shows the estimates of the P and T waves and of the local baseline, while Fig. 3(b) shows the P and T wave delineation results (i.e., estimated onset, peak, and end of each detected P and T wave). Note the close agreement of these estimation and delineation results with the ECG signal.

For a quantitative analysis, Table 1 presents the means (μ) and standard deviations (σ) of the differences between the automated delineation results and the manual annotations, for the proposed algorithm and for two alternative methods based on low-pass differentiation (LPD) [1] and wavelet transform (WT) [2]. These results were obtained using 1750 annotated ECG beats from the QTDB. It is seen that the proposed algorithm outperforms the other methods in terms of both detection sensitivity[1] and delineation accuracy.

6. CONCLUSION

We introduced a Bayesian model for the non-QRS intervals of ECG signals and proposed a block Gibbs sampler for joint delineation and waveform estimation of P and T waves. The block Gibbs sampler exploits the strong local dependencies in ECG signals. Validation using the annotated QT database showed that the proposed method provides reliable detection and accurate delineation for a wide variety of wave morphologies, and it outperforms two alternative methods. Our method also provides accurate waveform estimation, which makes it useful for T wave alternans analysis and other ECG analyses requiring wave morphology information.

[1]The sensitivity (also referred to as detection rate) is defined as $\mathrm{Se} \triangleq N_{\mathrm{TP}}/(N_{\mathrm{TP}}+N_{\mathrm{FN}})$, where N_{TP} is the number of true positive detections and N_{FN} is the number of false negative detections [2].

Table 1. Delineation and detection performance for QTDB

Parameter	Proposed alg.	LPD [1]	WT [2]
$\boldsymbol{b}_{\mathrm{P}}$: Se (%)	99.60	97.70	98.87
Onset-P: $\mu \pm \sigma$ (ms)	1.7 ± 10.8	14.0 ± 13.3	2.0 ± 14.8
Peak-P: $\mu \pm \sigma$ (ms)	2.7 ± 8.1	4.8 ± 10.6	3.6 ± 13.2
End-P: $\mu \pm \sigma$ (ms)	2.5 ± 11.2	-0.1 ± 12.3	1.9 ± 12.8
$\boldsymbol{b}_{\mathrm{T}}$: Se (%)	100	97.74	99.77
Onset-T: $\mu \pm \sigma$ (ms)	5.7 ± 16.5	N/A	N/A
Peak-T: $\mu \pm \sigma$ (ms)	0.7 ± 9.6	-7.2 ± 14.3	0.2 ± 13.9
End-T: $\mu \pm \sigma$ (ms)	2.7 ± 13.5	13.5 ± 27.0	-1.6 ± 18.1

7. REFERENCES

[1] P. Laguna, R. Jané, and P. Caminal, "Automatic detection of wave boundaries in multilead ECG signals: Validation with the CSE database," *Comput. Biomed. Res.*, vol. 27, no. 1, pp. 45–60, 1994.

[2] J. P. Martínez, R. Almeida, S. Olmos, A. P. Rocha, and P. Laguna, "A wavelet-based ECG delineator: Evaluation on standard databases," *IEEE Trans. Biomed. Eng.*, vol. 51, no. 4, pp. 570–581, 2004.

[3] V. S. Chouhan and S. S. Mehta, "Threshold-based detection of P and T-wave in ECG using new feature signal," *Int. J. Comp. Science Net. Security*, vol. 8, no. 2, pp. 144–152, 2008.

[4] J. P. Martínez and S. Olmos, "Methodological principles of T wave alternans analysis: A unified framework," *IEEE Trans. Biomed. Eng.*, vol. 52, no. 4, pp. 599–613, 2004.

[5] C. P. Robert and G. Casella, *Monte Carlo Statistical Methods*. New York: Springer, 2004.

[6] C. Lin, C. Mailhes, and J.-Y. Tourneret, "P- and T-wave delineation in ECG signals using a Bayesian approach and a partially collapsed Gibbs sampler," *IEEE Trans. Biomed. Eng.*, vol. 57, no. 12, pp. 2840–2849, Dec. 2010.

[7] P. Laguna, R. Mark, A. Goldberger, and G. Moody, "A database for evaluation of algorithms for measurement of QT and other waveform intervals in the ECG," *Comput. Cardiol.*, vol. 24, pp. 673–676, 1997.

[8] G. Kail, C. Novak, B. Hofer, and F. Hlawatsch, "A blind Monte Carlo detection-estimation method for optical coherence tomography," in *Proc. IEEE ICASSP-09*, Taipei, Taiwan, April 2009, pp. 493–496.

[9] R. Haas and J.-C. Belfiore, "A time-frequency well-localized pulse for multiple carrier transmission," *Wireless Personal Comm.*, vol. 5, pp. 1–18, 1997.

[10] F. Hlawatsch, *Time-Frequency Analysis and Synthesis of Linear Signal Spaces: Time-Frequency Filters, Signal Detection and Estimation, and Range-Doppler Estimation*. Boston (MA): Kluwer, 1998.

[11] V. S. Chouhan and S. S. Mehta, "Total removal of baseline drift from ECG signal," in *Proc. of the Int. Conf. on Computing: Theory and Applications*, Kolkata, India, March 2007, pp. 512–515.

[12] N. Dobigeon, J.-Y. Tourneret, and M. Davy, "Joint segmentation of piecewise constant autoregressive processes by using a hierarchical model and a Bayesian sampling approach," *IEEE Trans. Signal Process*, vol. 55, pp. 1251–1263, April 2007.

[13] J. Pan and W. J. Tompkins, "A real-time QRS detection algorithm," *IEEE Trans. Biomed. Eng.*, vol. 32, no. 3, pp. 230–236, 1985.